Optics and Lasers in Engineering 100 (2018) 216–225

Contents lists available at ScienceDirect

Optics and Lasers in Engineering

journal homepage: www.elsevier.com/locate/optlaseng

Non-iterative three dimensional reconstruction method of the structured light system based on polynomial distortion representation

Ping Zhou [a,*], Yunlei Yu [a], Weijia Cai [a,b], Siyuan He [a], Guangquan Zhou [a]

[a] School of Biological Science & Medical Engineering, Southeast University, Nanjing, 210096, China
[b] Suzhou Research Institute of Southeast University, Suzhou, 215123, China

ARTICLE INFO

Keywords:
Non-iterative
Reconstruction
Distortion
Projector model

ABSTRACT

In monocular structured light system, the iterative reconstruction method makes the measurement time-consuming, and the measurement accuracy is often hindered by the fact that the first-order radial distortion is included only. Compared with the conventional projector model, a new projector model, including both radial and tangential distortion, is proposed in this paper, which is described with the pinhole model according to the light direction. Furthermore, the iterative method is replaced by solving a quartic polynomial problem directly based on the proposed projector model. Experimental results show that the measurement accuracy and the efficiency are improved obviously. The standard deviation of the proposed method is 0.037mm, which is about a third of 0.113mm of the iterative method. The time consumed by the proposed method is 3.3% of that by the iterative method when one hundred thousand points are reconstructed.

1. Introduction

Structured light system is a three dimensional measurement system with high accuracy, simple equipment and satisfactory speed, which generally consists of one or more cameras and a projector [1,2]. It has been widely used in industrial precision inspection, three dimensional body scanning, heritage conservation, and so on [3–6]. The keys to a structured light system are system calibration, structured light encoding, and reconstruction. Many researchers contributed to these fields and made remarkable achievements.

As the most important problem, system calibration had been focused in the last decades [7–11]. Zhang solved the camera calibration accurately by observing a planar pattern [7], whose method had already been widely used in structured light system. Zhang and Huang treated the projector as an inverse camera [8], thus making the calibration of a projector the same as that of a camera. Then, Li et al. improved the projector calibration by reducing the phase error and interpolating the Digital Mirror Device (DMD) images [9]. To deal with the distortion, Huang et al. presented an error surface compensation method [10], which minimized mapping error caused by camera and projector distortion. Recently, Liu et al. proposed a projector calibration method by making use of photodiodes to directly detect the light emitted from a projector [11], and a polynomial distortion representation is employed to reduce the error of traditional projector model. Structured light encoding is another essential problem. Sinusoidal grating encoding and phase shifting algorithm are the most advanced and effective methods [12], by now they had already been utilized in most commercial structured light systems. An advanced topic of encoding is to reduce the number patterns for real-time measurement [13–15]. For example, Trusiak et al. proposed a hybrid single shot algorithm [14] for a composite structured light system, in which empirical mode decomposition was employed, aided by the principal components analysis, and He et al. reduced measurement error caused by spectrum overlapping [15] in a composite structured light system based on fringe parameter calculation. The final problem is reconstruction. Theoretically, reconstruction can be achieved directly based on optical triangle principle in the linear system model. However, there are two primary problems that make reconstruction more difficult, the phase error and the lens distortion. Numerous effective methods were proposed to reduce the phase error. Zhang and Yau improved the traditional look up table generation method [16] for the phase error by analyzing the captured fringe image of a flat board. Then, Liu et al. studied the gamma effect and developed a mathematical model [17] for predicting the effects of non-unitary gamma. Furthermore, Yatabe et al. proposed a post-processing method [18] for compensating general fringe distortion based on the inverse map estimation, which made the fringe patterns accurate enough. Lens distortion were also considered by many scholars [19–22], especially the first-order radial distortion. Valkenburg solved the reconstruction with iterative method [19] when including first-order radial distortion, which also gave a general description of reconstruction equations. Huang and Han simplified the iterative method [20] by undistorting the camera images firstly, and then solved the reconstruction with the first order radial distortion of projector. Ma et al. extended the reconstruction equations

* Corresponding author.
E-mail address: capzhou@163.com (P. Zhou).

http://dx.doi.org/10.1016/j.optlaseng.2017.08.013
Received 28 March 2017; Received in revised form 8 July 2017; Accepted 22 August 2017
Available online 6 September 2017
0143-8166/

to appropriate for complex distortion models [21], and corrected the error pixel by pixel based on iterative method. To make the measurement efficient, Li et al. eliminated the projector distortion by projecting distorted fringe patterns [22], which were generated according to the projector model. However, the solution to analytic reconstruction equations is always iterative and time-consuming, and the specific distortion model is also related to the measurement accuracy and efficiency. In a word, the lens distortion restricts the precision of structured light system and an appropriate non-iterative method is expected.

A non-iterative method is proposed in this paper to solve the lens distortion efficiently. This method is based on a projector model, which applies the pinhole model to the projector description according to the light direction. In this projector model, the measuring object is considered as the image plane, while the Digital Mirror Device (DMD) reflects light to it. Corresponding to this model, lens distortion description equations are reorganized, and the reconstruction is simplified to a problem of solving a polynomial. As the iteration is inevitable when the polynomial order exceeds four, the reconstruction is described by two polynomials of three order and four order, whose coefficients are obtained by curve fitting algorithm. The experimental results prove the validity of the proposed non-iterative method.

The rest of this paper is organized as follows: Section 2 describes the basic nonlinear model of structured light system. Section 3 discusses the proposed method, together with the ideas to it. In Section 4, experiments are implemented to verify the proposed method. Finally, Section 5 concludes this work.

2. Structured light system model

A monocular structured light system consists of a camera and a projector. The camera is described by a pinhole model, which is represented by intrinsic and extrinsic parameters, together with nonlinear compensation items to represent lens distortion [20]. The projector is generally considered as an inverse camera and it can capture DMD images [8], thus the camera model can be applied appropriately to the projector.

2.1. Camera and projector model

The pinhole model is described to present an ideal camera without lens distortion. M_c is an arbitrary point in the space with coordinates $X^w = [x^w, y^w, z^w]^T$ in the world coordinate system $\{O_W; X_W, Y_W, Z_W\}$, and $X^c = [x^c, y^c, z^c]^T$ in the camera coordinate system $\{O_C; X_C, Y_C, Z_C\}$, as shown in Fig. 1.

The relationship between M_c and its projection point m on the image plane $\{o; u, v\}$ is expressed as Eq. (1).

$$z^c \begin{bmatrix} u^c \\ v^c \\ 1 \end{bmatrix} = A^c \begin{bmatrix} R^c & T^c \end{bmatrix} X^w \tag{1}$$

where $[u^c, v^c, 1]^T$ is the homogeneous pixel coordinate of m in the image coordinate system $\{o; u, v\}$. A^c is the intrinsic parameters matrix of the camera, $[R^c \quad T^c]$ is the extrinsic parameters matrix that represents the rotation and translation between X^w and X^c. A^c and R^c are invertible matrices with 3×3 elements. T^c is a vector with 3×1 elements, expressed as $[t_1^c, t_2^c, t_3^c]^T$. A^c is expressed as Eq. (2).

$$A^c = \begin{bmatrix} \alpha^c & \gamma^c & u_0^c \\ 0 & \beta^c & v_0^c \\ 0 & 0 & 1 \end{bmatrix} \tag{2}$$

where $[u_0^c, v_0^c]^T$ is the principle point, α^c and β^c are the focal lengths along with the axes of the image plane, γ^c is the skew factor, normally set as zero.

On the basis of the pinhole model, lens distortion is included to improve the system accuracy. A typical lens distortion model including radial and tangential distortion is expressed as polynomials with normalized coordinate [23]. X_n^c is the normalized coordinate when lens distortion is ignored, which is expressed as Eq. (3).

$$X_n^c = [x_n^c, y_n^c]^T = \left[\frac{x^c}{z^c}, \frac{y^c}{z^c}\right]^T \tag{3}$$

When lens distortion is included, the normalized coordinate X_d^c is expressed as Eq. (4),

$$X_d^c = \begin{bmatrix} x_d^c \\ y_d^c \end{bmatrix} = LDF(X_n^c) = (1 + k_1^c r^2 + k_2^c r^4) X_n^c + D_t + O[(x_n^c, y_n^c)^5] \tag{4}$$

where LDF is the lens distortion function, k_1^c and k_2^c are radial distortion coefficients, D_t is the tangential distortion item caused by decentering distortion, r^2 is expressed as $r^2 = (x_n^c)^2 + (y_n^c)^2$. D_t is expressed as Eq. (5) [23].

$$D_t = \begin{bmatrix} p_1^c(3(x_n^c)^2 + (y_n^c)^2) + 2p_2^c x_n^c y_n^c \\ 2p_1^c x_n^c y_n^c + p_2^c((x_n^c)^2 + 3(y_n^c)^2) \end{bmatrix} \tag{5}$$

where p_1^c and p_2^c are tangential distortion coefficients. Therefore, the coordinate transformation process of nonlinear camera model is concluded as $X^w \to X^c \to X_n^c \to X_d^c \to ([u^c, v^c]^T)$.

In structured light system, the conventional projector model treats the projector as an inverse camera [9], whose emitted encoding patterns are imagined as the captured images. Thus the projector can capture a series of images and be modeled with the pinhole model. The coordinate transformation process of nonlinear projector model is specialized as $X^w \to X^p \to X_n^p \to X_d^p \to ([u^p, v^p]^T)$.

Here the superscript p means the projector coordinate. v^p is unknown to the structured light system [19]. Projecting enough encoding patterns in different directions will solve this problem easily, but it is not used in commercial systems because of time-consuming, increasing phase error and so on. Therefore, only u^p of a point on the emitter is available.

2.2. Iterative reconstruction method

Based on the pinhole model and Eq. (1), there are

$$\begin{aligned} z^c \begin{bmatrix} X_n^c \\ 1 \end{bmatrix} &= \begin{bmatrix} R^c & T^c \end{bmatrix} X^w \\ z^p \begin{bmatrix} X_n^p \\ 1 \end{bmatrix} &= \begin{bmatrix} R^p & T^p \end{bmatrix} X^w \end{aligned} \tag{6}$$

The relationship between X_n^c and X^p is deduced, expressed as Eq. (7),

$$z^c \begin{bmatrix} X_n^c \\ 1 \end{bmatrix} = \begin{bmatrix} R^c & T^c \end{bmatrix} \begin{bmatrix} R^p & T^p \end{bmatrix}^{-1} X^p \tag{7}$$

where $[R^p \quad T^p]^{-1}$ means the transformation from X^p to X^w rather than an actual inverse matrix. There are four unknowns, z^c and $X^p = [x^p, y^p, z^p]^T$, while only three linear equations are available in Eq. (7).

Considering the constraints provided by encoding patterns, there is

$$\frac{u^p - u_0^p}{\alpha^p} = LDF\left(\frac{x^p}{z^p}\right) \tag{8}$$

Combining Eq. (7) and Eq. (8), X^p and X^w can be solved theoretically. In view of the nonlinearity of Eq. (8), it generally is solved by iterative algorithm, such as a quasi-Newton strategy. It should be mentioned that the camera image point is undistorted directly regardless of the camera distortion models [20], thus only one non-linear equation, Eq. (8) appears in reconstruction to express the projector distortion.

3. Non-iterative reconstruction method

Although the iterative method is available, it is not always a good solution, especially when complex distortion model is included. Therefore, it is necessary to develop a non-iterative method for the reconstruction.

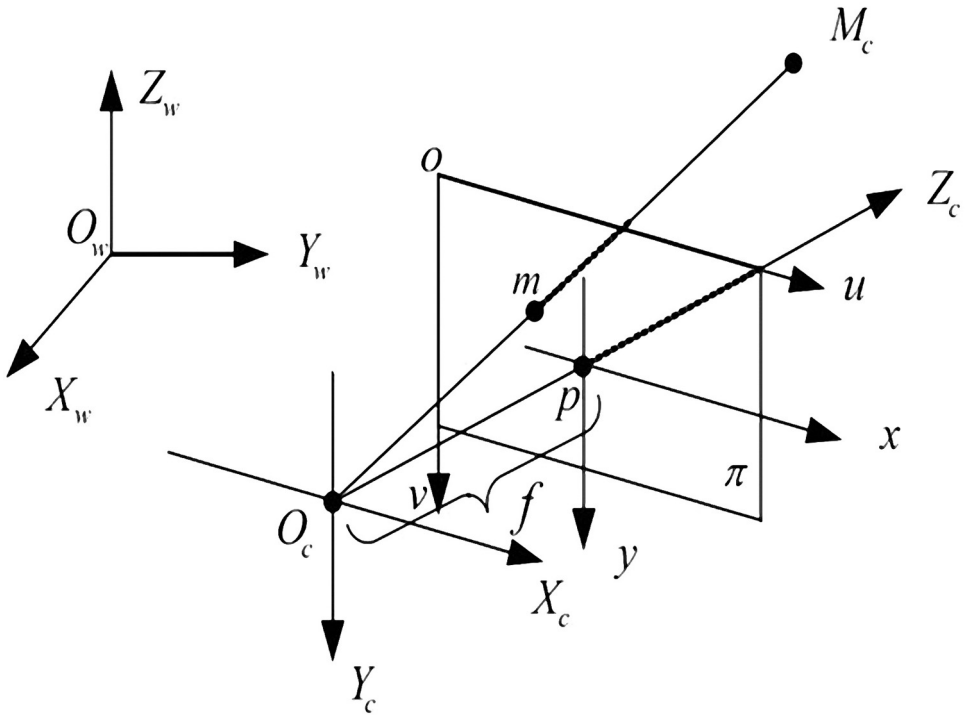

Fig. 1. The pinhole model of an ideal camera.

3.1. Basic solution

The non-iterative reconstruction method is also based on the combination of Eq. (7) and Eq. (8) when only k_1^p is included. An idea to the problem is expressing x^p, y^p, z^p with z^c firstly and then eliminating them in Eq. (8). Therefore, the reconstruction is solving a cubic equation with unknown z^c. The particular scheme is expressed as follows.

Based on the invertibility of linear equations, Eq. (7) is replaced by Eq. (9).

$$\begin{bmatrix} x^p \\ y^p \\ z^p \end{bmatrix} = M \begin{bmatrix} z^c x_n^c \\ z^c y_n^c \\ z^c \end{bmatrix} + \eta \tag{9}$$

where

$$\begin{aligned} M &= \begin{bmatrix} m_1 & m_2 & m_3 \\ m_4 & m_5 & m_6 \\ m_7 & m_8 & m_9 \end{bmatrix} = R^p (R^c)^{-1} \\ \eta &= \begin{bmatrix} \eta_1 \\ \eta_2 \\ \eta_3 \end{bmatrix} = R^p (R^c)^{-1} T^c + T^p \end{aligned} \tag{10}$$

As mentioned above, Eq. (8) is replaced by Eq. (11) when x^p, y^p, z^p in Eq. (8) is eliminated.

$$a_0 = \left\{ 1 + k_1^p \left[\left(\frac{a_1 z^c + \eta_1}{a_3 z^c + \eta_3} \right)^2 + \left(\frac{a_2 z^c + \eta_2}{a_3 z^c + \eta_3} \right)^2 \right] \right\} \frac{a_1 z^c + \eta_1}{a_3 z^c + \eta_3} \tag{11}$$

where

$$\begin{aligned} a_0 &= \frac{u^p - u_0^p}{\alpha^p} \\ a_1 &= (m_1 x_n^c + m_2 y_n^c + m_3) \\ a_2 &= (m_4 x_n^c + m_5 y_n^c + m_6) \\ a_3 &= (m_7 x_n^c + m_8 y_n^c + m_9) \end{aligned} \tag{12}$$

It can be seen from Eq. (12) that a_0, a_1, a_2, a_3 are constants determined by system parameters and image coordinates. Eq. (11) is actually a cubic equation, and can be solved by available formulas directly, which is expressed by Eq. (13).

$$a_0 (a_3 z^c + \eta_3)^3 = \left\{ (a_3 z^c + \eta_3)^2 + k_1^p \left[(a_1 z^c + \eta_1)^2 + (a_2 z^c + \eta_2)^2 \right] \right\} (a_1 z^c + \eta_1) \tag{13}$$

The meaning of Eq. (13) is depicted in Fig. 2. The reconstruction without projector distortion is shown in Fig. 2(a), while the reconstruction considering k_1^p is shown in Fig. 2(b). More specifically, Eq. (6) is represented with the line l_0 in Fig. 2, Eq. (8) is represented with π_k in Fig. 2(b) or π_0 in Fig. 2(a), depending on whether the projector distortion is included or not. Therefore, the intersection of l_0 and π_0/π_k is the reconstructed object P, and Eq. (13) is represented by the dotted line in Fig. 2(b), commented as "*Cubic curve in* Eq. (13)" .

So far a non-iterative solution to the reconstruction is built and described as the following steps:

(1) $(R^p, R^c, t^c, t^p) \rightarrow (M, \eta)$;
(2) $([x_d^c, y_d^c]^T, k_1^c) \rightarrow ([x_n^c, y_n^c]^T)$;
(3) $([x_n^c, y_n^c]^T, M) \rightarrow (a_0, a_1, a_2, a_3)$;
(4) $(a_0, a_1, a_2, a_3, k_1^p, \eta) \rightarrow z^c$;
(5) $([x_n^c, y_n^c]^T, z^c) \rightarrow ([x^w, y^w, z^w])$.

Although the non-iterative reconstruction method is developed when k_1^p is included, it is still not an adaptive method when more projection distortion parameters are considered. Different projector distortion parameters lead to different polynomials, and result in different equations to be solved. For example, k_1^p leads to Eq. (11) and results in Eq. (13) to be solved. When k_2^p, p_1^p, and p_2^p are included, the solution becomes intricate extremely and even more time-consuming than an iterative method. In addition, k_2^p results in quintic equation, which has been proved analytically unsolvable, thus an iterative method is inevitable.

3.2. Improved solution

The basic solution described in the last section is not appropriate in all cases, but it provides us an excellent idea to deal with the reconstruction. It is deduced that the reconstruction can be simplified to the problem of solving a polynomial. Therefore, an outlet for the reconstruction is to find a polynomial to approximate Eq. (13).

A new projector model is proposed to implement our idea, as shown in Fig. 3. The pinhole model of camera is shown in Fig. 3(a), in which an object P maps to a pixel p on image plane along with the light direction. The conventional projector model based on the pinhole model is shown

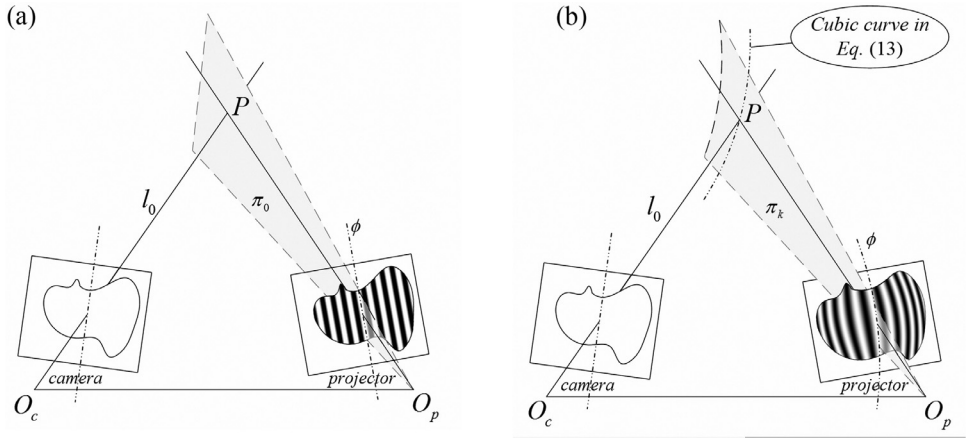

Fig. 2. The reconstruction of the structured light system. (a) the reconstruction without projector distortion; (b) the reconstruction when k_1^p is included.

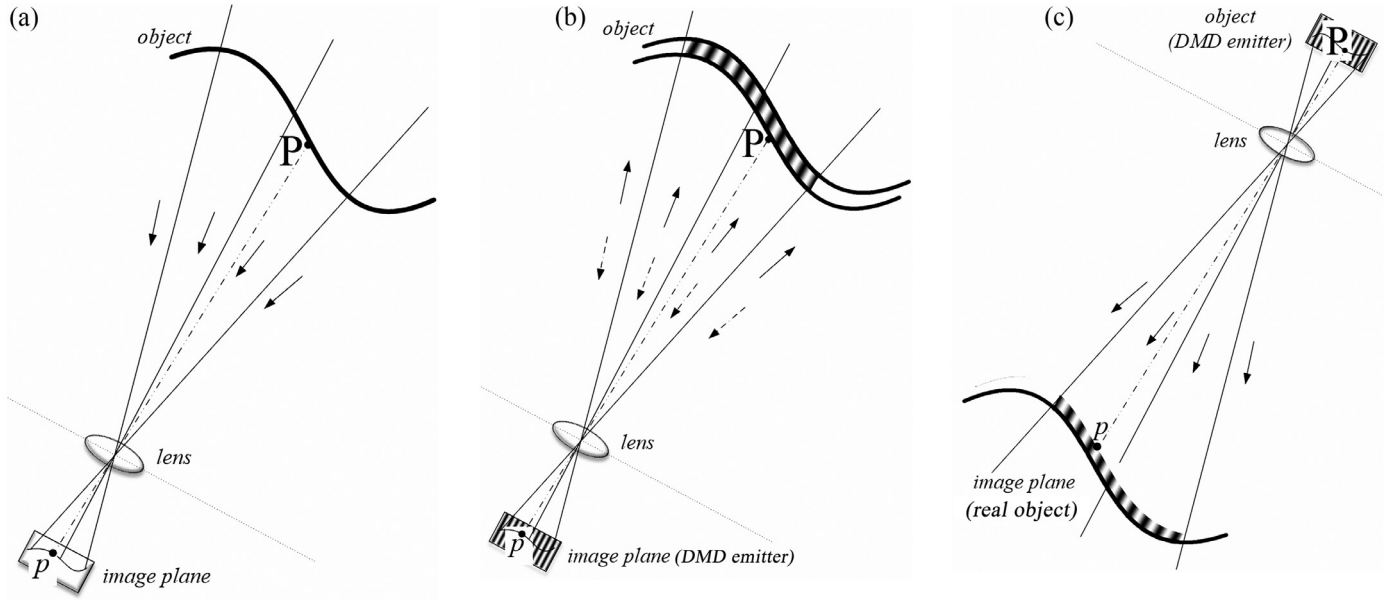

Fig. 3. Pinhole models in the structured light system. (a) the pinhole model of camera; (b) the conventional projector model; (c) the proposed projector model.

in Fig. 3(b). The projector is considered as an inverse camera, the solid and dashed arrows indicate the actual and assumed light direction in pinhole model respectively. In this model, the DMD is image plane and the object projects its structured light patterns onto DMD, along with the assumed light direction. The proposed projector model is shown in Fig. 3(c), where the pinhole model is applied to describe the projector according to the actual light direction. Specially, the DMD is considered as the object in the pinhole model, and it reflects the light to the real object, the image plane in Fig. 3(c), even though it is not an image plane. In other words, an assumed object P on DMD maps to a point p on real object.

To simplify the reconstruction, the projector distortion description equations are reorganized corresponding to the proposed projector model, which are depicted as Eq. (14).

$$\begin{aligned} X_n^p &= \begin{bmatrix} x_n^p \\ y_n^p \end{bmatrix} = \overline{LDF}(X_d^p) = (1 + \overline{k_1^p} r_d^2 + \overline{k_2^p} r_d^4) X_d^p + \overline{D_t} + O[(x_d^p, y_d^p)^5] \\ \overline{D_t} &= \begin{bmatrix} \overline{p_1^p}(3(x_d^p)^2 + (y_d^p)^2) + 2\overline{p_2^p} x_d^p y_d^p \\ 2\overline{p_1^p} x_d^p y_d^p + \overline{p_2^p}((x_d^p)^2 + 3(y_d^p)^2) \end{bmatrix} \end{aligned} \tag{14}$$

where $\overline{LDF}$ is the lens distortion function of the proposed projector model, $r_d^2 = (x_d^p)^2 + (y_d^p)^2$, X_n^p is the normalized distorted coordinate when the proposed projector distortion parameters $(\overline{k_1^p}, \overline{k_2^p}, \overline{p_1^p}, \overline{p_2^p})$ are included, whose meaning is the same as the normalized undistorted coordinate in Eq. (3). X_d^p is the normalized undistorted coordinate when $(\overline{k_1^p}, \overline{k_2^p}, \overline{p_1^p}, \overline{p_2^p})$ are included, whose meaning is the same as the normalized distorted coordinate in Eq. (4). It is obvious that the proposed projector model in Fig. 3(c) is the inverse of the model in Fig. 3(b), thus the X_n^p in Fig. 3(c) is the X_d^p in Fig. 3(b) and vice versa. It should be mentioned that $(k_1^p, k_2^p, p_1^p, p_2^p)$ is generally unequal to $(\overline{k_1^p}, \overline{k_2^p}, \overline{p_1^p}, \overline{p_2^p})$. Actually, the two groups of distortion parameters, $(k_1^p, k_2^p, p_1^p, p_2^p)$ and $(\overline{k_1^p}, \overline{k_2^p}, \overline{p_1^p}, \overline{p_2^p})$ formulize two processes of projector coordinate transformation, $X_d^p \rightarrow X_n^p$ and $X_n^p \rightarrow X_d^p$. When the proposed projector model is applied, the calibration is implemented by the linear least squares method to obtain the proposed projector distortion parameters.

Apart from the new projector model, phase constraint provided by encoding patterns is essential to the improved solution. The reconstruction is expressed as $(([x_d^c, y_d^c]^T \rightarrow [x_n^c, y_n^c]^T), \phi) \rightarrow ([x^w, y^w, z^w])$ when the projector distortion is ignored, where the phase ϕ is expressed by the dash-dotted line on the projector image plane, as shown in Fig. 2(a). In another perspective, when the projector distortion is included, ϕ is the dash-dotted curve on the projector image plane as shown in Fig. 2(b),

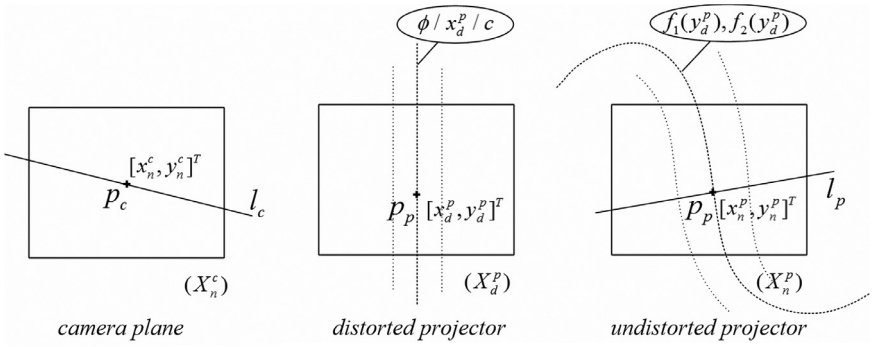

Fig. 4. The matching of corresponding points based on the epipolar constraint when the projector distortion is included.

expressed as x_n^p. Furthermore, ϕ is also a dashed straight line on the projector image plane, but expressed as x_d^p. Therefore, the reconstruction can be considered as the intersection of l_0 and π_k in Fig. 2(b), it can also be considered as the process to find the matching position along with the straight phase line.

The improved solution is now available to the reconstruction. Based on the phase constraint, ϕ and x_d^p are calculated directly. It is known that the matching position is located at the phase line, ϕ or x_d^p. Setting x_d^p as a known constant c and eliminating it in Eq. (14), equations with y_d^p unknown are expressed as Eq. (15).

$$\begin{aligned} x_n^p &= (1 + \overline{k_1^p}(c^2 + (y_d^p)^2) + \overline{k_2^p}(c^2 + (y_d^p)^2)^2)c + \overline{p_1^p}(3c^2 + (y_d^p)^2) + 2\overline{p_2^p}cy_d^p \\ y_n^p &= (1 + \overline{k_1^p}(c^2 + (y_d^p)^2) + \overline{k_2^p}(c^2 + (y_d^p)^2)^2)y_d^p + 2\overline{p_1^p}cy_d^p + \overline{p_2^p}(c^2 + 3(y_d^p)^2) \end{aligned} \tag{15}$$

It is obvious that Eq. (15) is expressed as two polynomials, and $[x_n^p, y_n^p]^T$ is the matching position to be solved. As y_d^p is unknown, unfortunately, Eq. (15) can not be solved directly, so an additional constraint is required. In this paper, the epipolar constraint [24] is applied, which is the straight line on projector image plane corresponding to any $[x_n^c, y_n^c]^T$. An epipolar pair is shown in Fig. 4. For a point p_c in camera image plane, the epipolar pair is l_c and l_p. Moreover, p_p is always located at l_p. Assuming l_p is expressed as Eq. (16), the parameters (A, B, C) of Eq. (16) are deduced with $[x_n^c, y_n^c]^T$ and $[R^c \quad T^c]$.

$$Ax_n^p + By_n^p + C = 0 \tag{16}$$

Let us rewrite Eq. (15) to a compact form, Eq. (17).

$$\begin{aligned} x_n^p &= f_1(y_d^p) \\ y_n^p &= f_2(y_d^p) \end{aligned} \tag{17}$$

where f_1 and f_2 are polynomials with unknown y_d^p. Combining Eq. (16) and Eq. (17), $[x_n^p, y_n^p]^T$ is eliminated and a polynomial with only y_d^p unknown is obtained, expressed as Eq. (18). The reconstruction is implemented after acquiring the matching position $[x_d^p, y_d^p]^T$ by solving Eq. (18) directly.

$$Af_1(y_d^p) + Bf_2(y_d^p) + C = 0 \tag{18}$$

The reconstruction is described as the following steps:

(1) $([x_d^p, y_d^p]^T, [x_n^p, y_n^p]^T) \rightarrow (\overline{k_1^p}, \overline{k_2^p}, \overline{p_1^p}, \overline{p_2^p})$;
(2) $([x_d^c, y_d^c]^T) \rightarrow \phi \rightarrow (x_d^p = c)$;
(3) $([x_n^c, y_n^c]^T, [R^c, T^c]) \rightarrow (A, B, C)$;
(4) $((\overline{k_1^p}, \overline{k_2^p}, \overline{p_1^p}, \overline{p_2^p}), c) \rightarrow (f_1, f_2)$;
(5) $((A, B, C), (f_1, f_2)) \rightarrow y_d^p$;
(6) $([x_d^c, y_d^c]^T, [x_d^p, y_d^p]^T) \rightarrow ([x^w, y^w, z^w])$.

However, it is still not an ideal method for the reconstruction as iteration is inevitable when k_2^p is included and Eq. (18) is quintic. Moreover, the estimation of $(\overline{k_1^p}, \overline{k_2^p}, \overline{p_1^p}, \overline{p_2^p})$ introduces accumulated error, which reduces the reconstruction accuracy. Taking Eq. (15) into consideration again, it actually expresses the projector distortion with polynomials. Therefore, Eq. (17) reveals the essence that f_1 and f_2 describe the relation between $[x_d^p, y_d^p]^T$ and $[x_n^p, y_n^p]^T$, which is appropriated by the polynomials, as illustrated in Fig. 4. The dotted curves of distorted projector in Fig. 4 are described by Eq. (17). l_p is the corresponding epipolar of l_c described by Eq. (16). Therefore, the reconstruction is simplified by approximating f_1 and f_2 with specific polynomials, rather than Eq. (15).

As depicted in Eq. (15), f_1 is a quartic function, while f_2 is quintic. A further analysis to Fig. 4 also manifests that f_1 is always one order lower than f_2, which is intelligible because x_d^p is constant, while y_d^p is unknown. If the order of f_1 or f_2 is given, the corresponding polynomials can be fitted with the least squares method. To avoid the iteration, f_1 is fitted with a cubic polynomial and f_2 is with quartic, expressed as Eq. (19).

$$\begin{aligned} x_n^p &= b_0 + b_1(y_d^p) + b_2(y_d^p)^2 + b_3(y_d^p)^3 \\ y_n^p &= d_0 + d_1(y_d^p) + d_2(y_d^p)^2 + d_3(y_d^p)^3 + d_4(y_d^p)^4 \end{aligned} \tag{19}$$

where (b_0, b_1, b_2, b_3) and $(d_0, d_1, d_2, d_3, d_4)$ are coefficients to be fitted. Generally, there are always hundreds of points for a specific x_d^p so that Eq. (19) can always be fitted correctly. Combining Eq. (19) and Eq. (16), the corresponding y_d^p can be solved by Eq. (20).

$$e_0 + e_1(y_d^p) + e_2(y_d^p)^2 + e_3(y_d^p)^3 + e_4(y_d^p)^4 = 0 \tag{20}$$

where

$$\begin{aligned} e_0 &= Ab_0 + Bd_0 + C \\ e_1 &= Ab_1 + Bd_1 \\ e_2 &= Ab_2 + Bd_2 \\ e_3 &= Ab_3 + Bd_3 \\ e_4 &= Bd_4 \end{aligned} \tag{21}$$

The reconstruction is implemented by now with the polynomial in Eq. (20). Iteration and unnecessary accumulated error are avoided in the reconstruction. The pipeline is described as the following steps:

(1) $([x_d^c, y_d^c]^T) \rightarrow \phi \rightarrow (x_d^p = c)$;
(2) $(y_d^p, [x_n^p, y_n^p]^T) \rightarrow ((b_0, b_1, \ldots), (d_0, d_1, \ldots))$;
(3) $([x_n^c, y_n^c]^T, [R^c, T^c]) \rightarrow (A, B, C)$;
(4) $((b_0, b_1, \ldots), (d_0, d_1, \ldots), (A, B, C)) \rightarrow (e_0, e_1, \ldots)$;
(5) $(e_0, e_1, \ldots) \rightarrow y_d^p$;
(6) $([x_d^c, y_d^c]^T, [x_d^p, y_d^p]^T) \rightarrow ([x^w, y^w, z^w])$.

In fact, there is still a minor problem in Eq. (20) that it always gives four primitive solutions, but only one of them is correct. A pair of complex roots and a pair of real roots can be found for Eq. (20), the correct solution can be picked out easily from the pair of real roots when restricted by the valid field (the resolution of DMD images).

4. Experimental results

To verify the proposed method, a calibration board with 64 circle centers, shown in Fig. 5, is measured by the monocular structured light

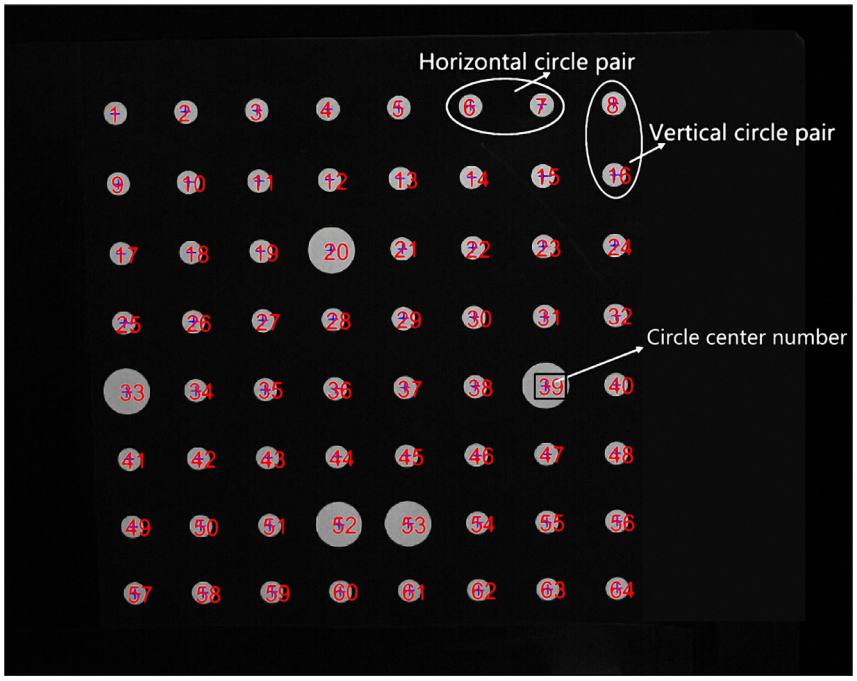

Fig. 5. Calibration board with 64 circle centers.

Table 1
The error comparison of the iterative method and the proposed method. (unit: *mm*).

		Error estimation with circle pair distances		*Error estimation with circle centers*
		Standard deviation	*80% marking line*	*Standard deviation*
The iterative method	$(\overline{k_1^p})$	0.1129	0.1419	0.5769
The proposed method	$(\overline{k_1^p}, \overline{k_2^p}, \overline{p_1^p}, \overline{p_2^p})$ *Polynomial order*: 4	0.0373	0.0507	0.1479
	$(\overline{k_1^p}, \overline{k_2^p}, \overline{p_1^p}, \overline{p_2^p})$ *Polynomial order*: 5	0.0374	0.0512	0.1474
	$(\overline{k_1^p}, \overline{k_2^p}, \overline{k_3^p}, \overline{p_1^p}, \overline{p_2^p})$ *Polynomial order*: 7	0.0374	0.0501	0.1511

system we constructed, which is equipped with a projector, BENQ GP1, working at 896*896, and a camera, MV-VD 120SC, shooting at a total of 1280*960 pixels. The circle centers are numbered from 1 to 64 ("circle center number" in Fig. 5), and the distance between circle centers ("horizontal/vertical circle pair" distance in Fig. 5) is 30 mm with the error of ± 0.005 mm.

The circle centers on the calibration board are measured by the iterative method and the proposed non-iterative method respectively. The measurement error of circle pair distance is shown in Fig. 6, and the distance from circle centers to the fitting plane of calibration board is shown in Fig. 7.

The measurement error of the iterative method is shown in Fig. 6(a) and that of the proposed method is shown in Fig. 6(b) on the same scale. It is obvious that the error in Fig. 6(b) is less than the error in Fig. 6(a). Some estimation parameters, including standard deviation and 80% marking line are calculated to make the comparison concrete, as depicted in Table 1. The 80% marking line is a positive threshold higher than 80% circle pair absolute distances while lower than 20% circle pair absolute distances. The error of the iterative method is about three times higher than that of the proposed method, regardless of both the standard derivation and the 80% marking line.

The 64 reconstructed circle centers are coplanar, thus the distances from the reconstructed circle centers to the fitting plane are considered as the measurement error, which are shown in Fig. 7. The error of the iterative method and the proposed method are plotted in Fig. 7(a) and Fig. 7(b) respectively, and trend lines are fitted with polynomials to reveal the residual error. The standard deviations of Fig. 7 are also calculated and listed in Table 1. It can be seen from Fig. 7 and Table 1 that the standard deviation of the iterative method is about four times higher than that of the proposed method. The trend lines in Fig. 7 also indicate that the lens distortion is not corrected completely by the iterative method, but almost corrected completely by the proposed method.

More experiments are conducted to further verify the proposed method. The circle centers are reconstructed with the proposed method in different conditions and the measurement error is shown in Fig. 8. The error shown in Fig. 8(a) and Fig. 8(b) is the same as that in Fig. 6(b) and Fig. 7(b), which is estimated by using the reconstructed circle centers when $(\overline{k_1^p}, \overline{k_2^p}, \overline{p_1^p}, \overline{p_2^p})$ is included and a quartic polynomial is fitted in reconstruction. In comparison to the Fig. 8(a) and Fig. 8(b), the error shown in Fig. 8(c) and Fig. 8(d) is estimated when a quintic polynomial is fitted, while the error shown in Fig. 8(e) and Fig. 8(f) is estimated when $(\overline{k_1^p}, \overline{k_2^p}, \overline{k_3^p}, \overline{p_1^p}, \overline{p_2^p})$ is included and a seven order polynomial is fitted. Here $\overline{k_3^p}$ is the third-order radial distortion of the projector, an item of Eq. (14), which is expressed as $\overline{k_3^p} r_d^6$. The standard deviation and 80% marking line of Fig. 8 are also listed in Table 1. It can be seen from Fig. 8 and Table 1 that the measurement error of the proposed method is almost the same, and a higher order polynomial or additional distortion parameters does not improve the performance significantly. Therefore, a quartic polynomial is appropriate for the proposed method and $(\overline{k_1^p}, \overline{k_2^p}, \overline{p_1^p}, \overline{p_2^p})$ is sufficient for the projector distortion.

Above all, the proposed method improves the performance of the monocular structured light system obviously, which corrects the projector's lens distortion dramatically by introducing the tangential distortion and avoids the iteration by constructing a quartic polynomial. The experimental results also demonstrate that a quartic polynomial is

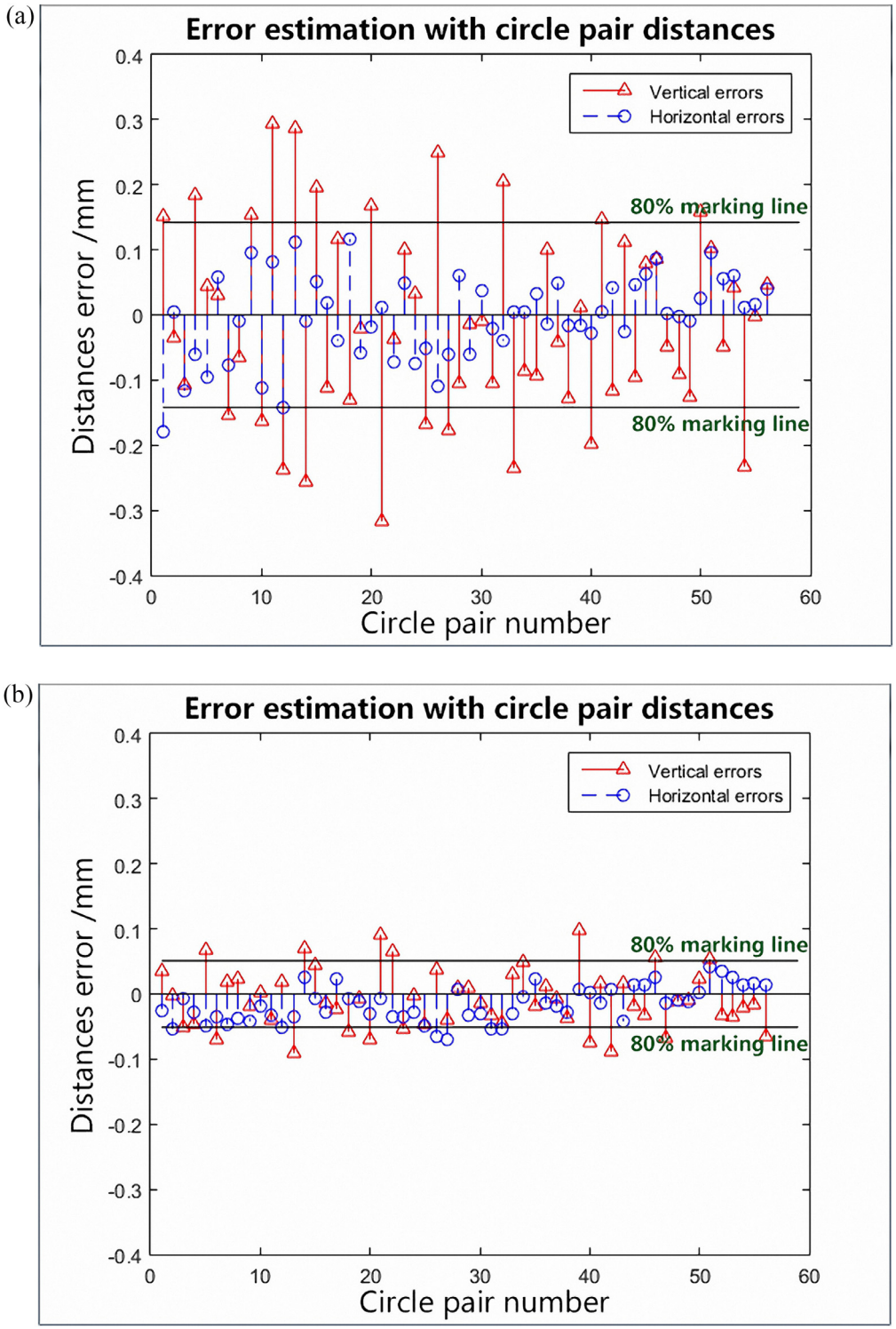

Fig. 6. Error estimation with circle pair distances. (a) the iterative method. (b) the proposed method.

appropriate and the tangential distortion is necessary for the structured light system.

Some objects are measured to verify the efficiency of the proposed method, including a boy sculpture and a pair of hands. The measurement results with the proposed method are rendered and shown in Fig. 9. It is obvious that the proposed method reserves most details of the sculpture and the hands, and loses almost no points except for the shading area.

The boy sculpture in Fig. 9 is rendered with 102,249 points. As an example to compare the efficiency of two methods, the boy sculpture is also reconstructed by the iterative method on the same computer. The consumed time are 14.637 seconds and 445.959 seconds when reconstructed by the proposed method and the iterative method respectively. It can be deduced that the proposed method consumes 3.28% of the time used by the iterative method. In addition, the hands in Fig. 9, rendered with 81,509 points, are also reconstructed with the above methods, and the corresponding consumed times are 11.784 seconds and 352.468 seconds. Therefore, the proposed method consumes 3.34% of the time used by the iterative method. In conclusion, the experimental results demon-

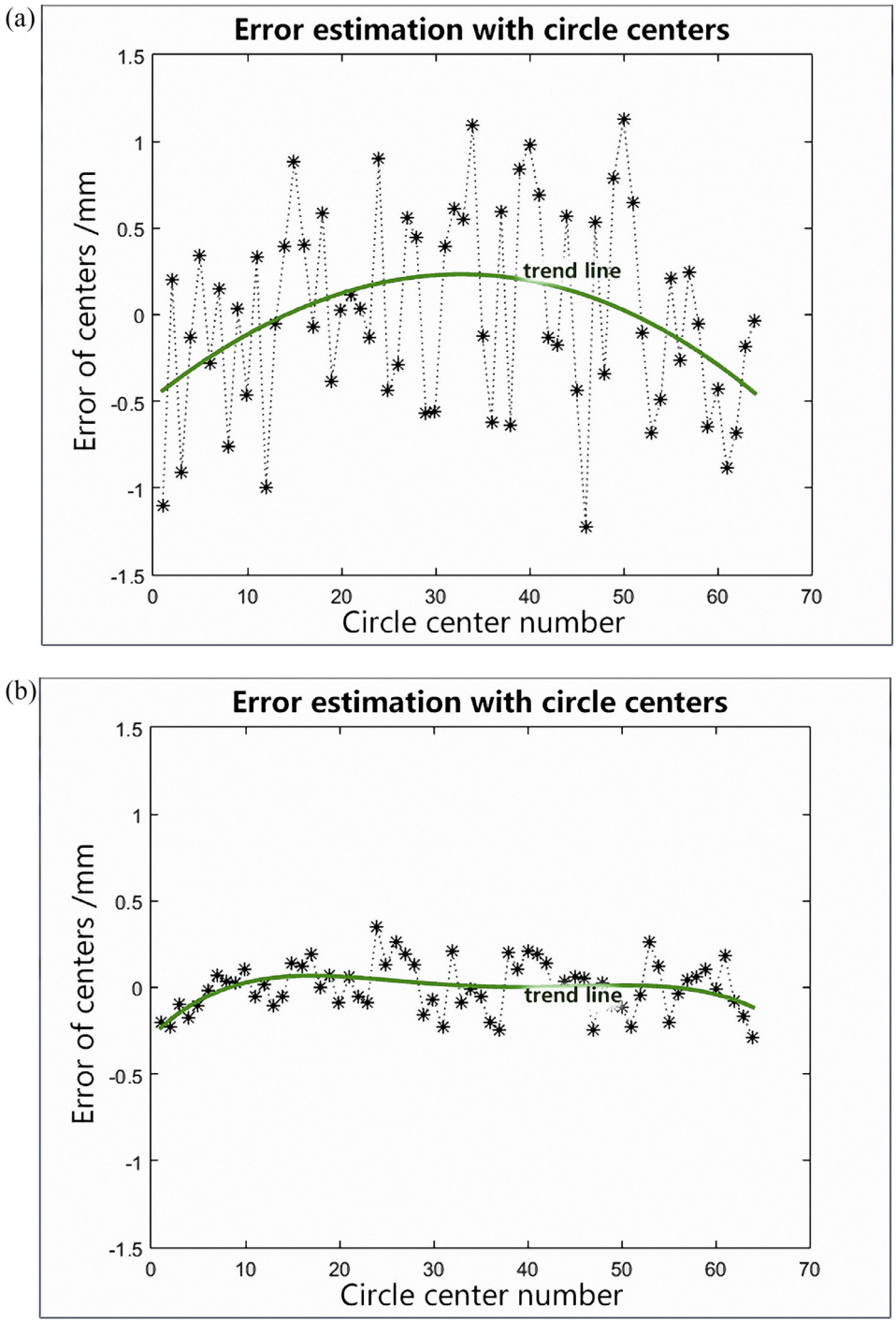

Fig. 7. Error estimation with circle centers. (a) the iterative method; (b) the proposed method.

strate that the proposed method is of good efficiency, and it consumes 3.3% of the time consumed by the iterative method when one hundred thousand points are reconstructed.

5. Conclusions

Reconstruction is one of the most important problems of the structured light system. In most cases, iterative method is applied in reconstruction with only first-order radial distortion included, which is not accurate enough and time-consuming. In consideration of these disadvantages, a non-iterative and accurate method is proposed in this paper to implement the reconstruction. The proposed method describes the projector with the pinhole model according to the light direction, and then simplifies the reconstruction to a problem of solving a quartic polynomial. There are two important distinctions in the proposed method. Firstly, they analyze the projector model in a completely different way. Secondly, compared to the iterative method, the proposed method takes the tangential distortion of the projector into consideration to improve the measurement accuracy, and avoids the iteration by constructing a quartic polynomial. The experimental results show that the measurement accuracy and the efficiency are improved obviously. However, as more than one pattern are usually used in the structured light system to achieve satisfied measurement accuracy, it is essential to improve the encoding method to make the structured light system real-

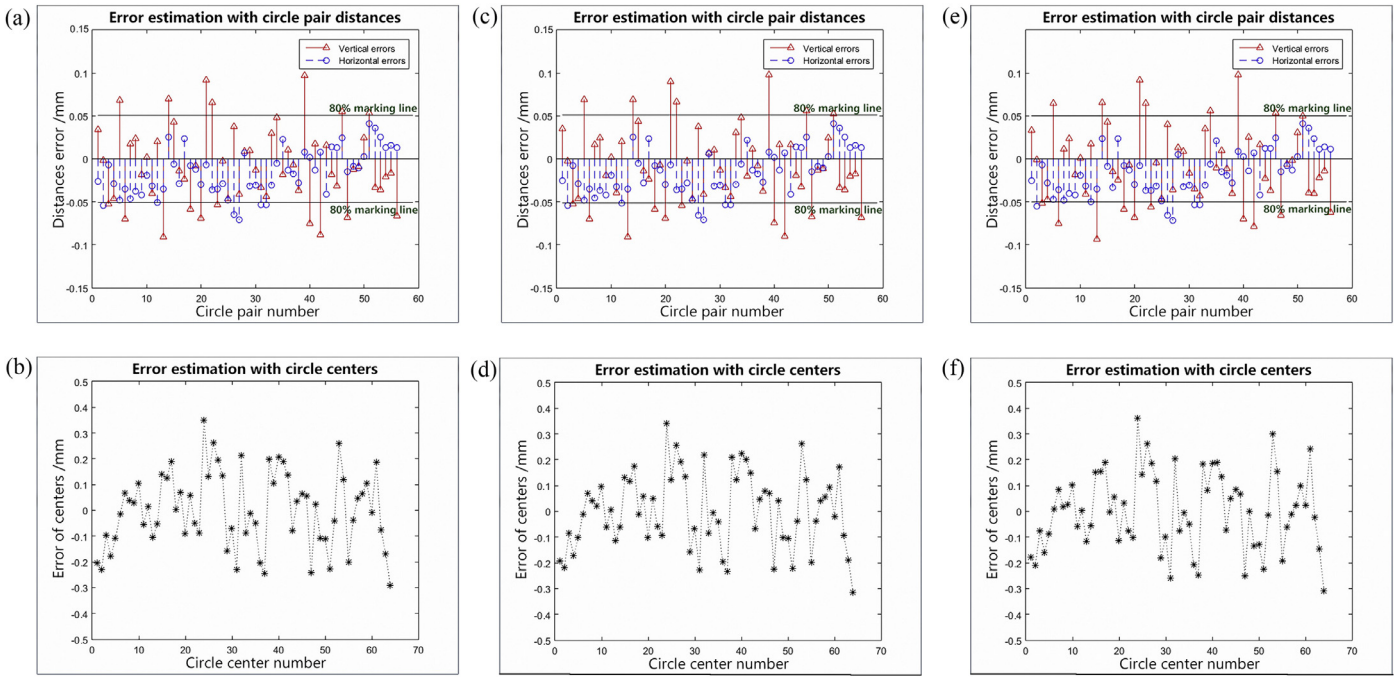

Fig. 8. Error estimation of the proposed method in different conditions. (a) and (b) error estimation when $(\overline{k_1^p}, \overline{k_2^p}, \overline{p_1^p}, \overline{p_2^p})$ is included and a quartic polynomial is fitted; (c) and (d) error estimation when $(\overline{k_1^p}, \overline{k_2^p}, \overline{p_1^p}, \overline{p_2^p})$ is included and a quintic polynomial is fitted; (e) and (f) error estimation when $(\overline{k_1^p}, \overline{k_2^p}, \overline{k_3^p}, \overline{p_1^p}, \overline{p_2^p})$ is included and a seven order polynomial is fitted.

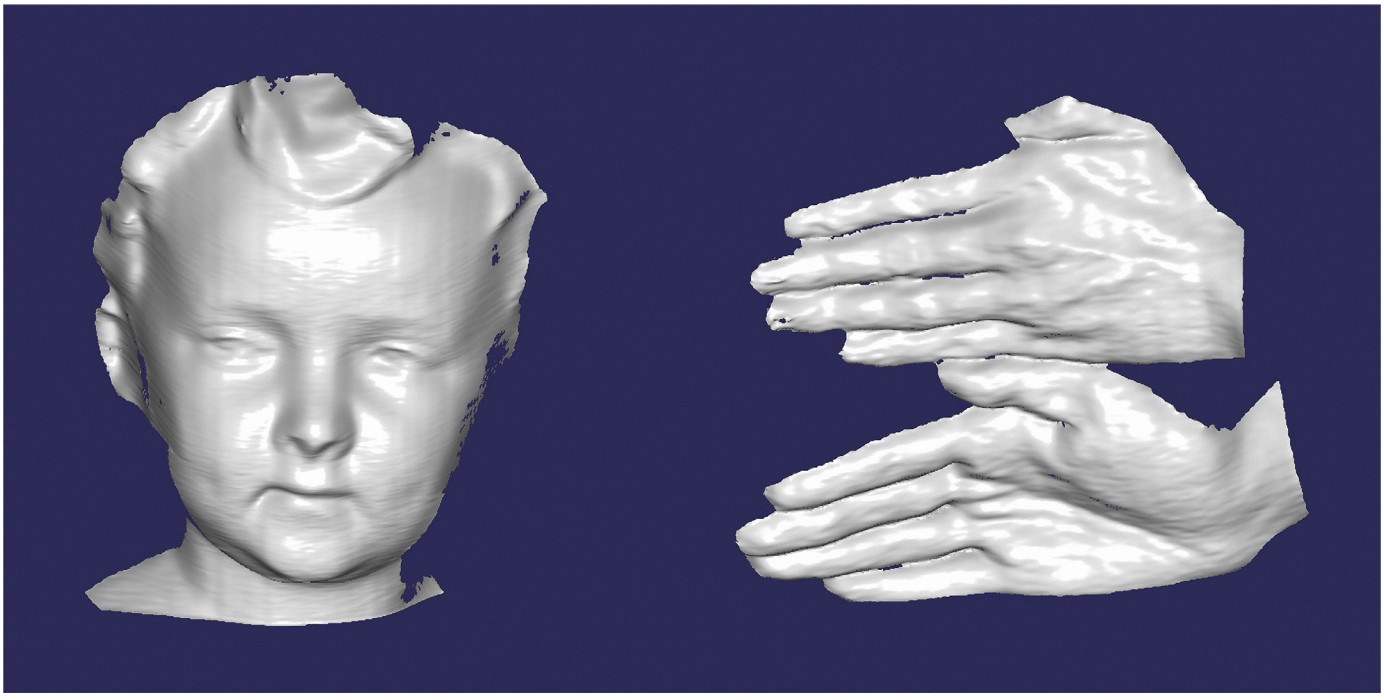

Fig. 9. The rendered reconstruction results of real objects.

time. If an accurate and universal single shot fringe projection method is developed, real-time reconstruction could be expected with the reconstruction method proposed in this paper.

Acknowledgment

This work was supported by the National Natural Science Foundation of China (11572087) and the National Natural Science Foundation of China (3207037434).

References

[1] Zhang S. Recent progresses on real-time 3D shape measurement using digital fringe projection techniques. Opt Laser Eng 2010;48(2):149–58.
[2] Jeught SVD, Dirckx JJJ. Real-time structured light profilometry: a review. Opt Laser Eng 2016;87:18–31.
[3] Ferraq Y, Black D, Lagarde JM, Schmitt AM, Dahan S, Grolleau JL JL, et al. Use of a 3D imaging technique for non-invasive monitoring of the depth of experimentally induced wounds. Skin Res Technol 2007;13(4):399–405.
[4] Liu S, Tan Q, Zhang Y. Shaft diameter measurement using structured light vision. Sensors 2015;15(8):19750–67.

[5] Bøgh SM, Grüner HS, Kjær R, Allin T, Linde JM. 3D-imaging: a scanning light pattern projector. Appl Opt 2016;55(32):9074.
[6] Pösch A, Schlobohm J, Matthias S, Reithmeier E. Rigid and flexible endoscopes for three dimensional measurement of inside machine parts using fringe projection. Opt Laser Eng 2017;89:178–83.
[7] Zhang Z. A flexible new technique for camera calibration. IEEE T Pattern Anal 2000;22(11):1330–4.
[8] Zhang S, Huang P. Novel method for structured light system calibration. Opt Eng 2006;45(8) 083601-083601-8.
[9] Li Z, Shi Y, Wang C, Wang Y. Accurate calibration method for a structured light system. Opt Eng 2008;47(5) 053604-053604-9.
[10] Huang J, Wang Z, Gao J, Xue Q. Projector calibration with error surface compensation method in the structured light three-dimensional measurement system. Opt Eng 2013;52(4) 043602-043602.
[11] Liu M, Sun C, Huang S, Zhang Z. An accurate projector calibration method based on polynomial distortion representation. Sensors 2015;15(10):26567–82.
[12] Song L, Dong X, Xi J, Yu Y, Yang C. A new phase unwrapping algorithm based on three wavelength phase shift profilometry method. Opt Laser Technol 2013;45:319–29.
[13] Zhang Z. Review of single shot 3D shape measurement by phase calculation-based fringe projection techniques. Opt Laser Eng 2012;50(8):1097–106.
[14] Trusiak M, Służewski Ł, Patorski K. Single shot fringe pattern phase demodulation using Hilbert-Huang transform aided by the principal component analysis. Opt Express 2016;24(4):4221.
[15] He Y, Cao Y. A composite-structured-light 3D measurement method based on fringe parameter calibration. Opt Laser Eng 2011;49(7):773–9.
[16] Zhang S, Yau S. Generic non-sinusoidal phase error correction for three dimensional shape measurement using a digital video projector. Appl Opt 2007;46(1):36–43.
[17] Liu K, Wang Y, Lau DL, Hao Q, Hassebrook LG. Gamma model and its analysis for phase measuring profilometry. JOSA A. 2010;27(3):553–62.
[18] Yatabe K, Ishikawa K, Oikawa Y. Compensation of fringe distortion for phase-shifting three-dimensional shape measurement by inverse map estimation. Appl Opt 2016;55(22):6017.
[19] Valkenburg RJ, McIvor AM. Accurate 3D measurement using a structured light system. Image Vision Comput 1998;16(2):99–110.
[20] Huang P, Han X. On improving the accuracy of structured light systems. Optics East 2006 SPIE. 2006; 63820H-63820H-8.
[21] Ma S, Zhu R, Quan C, Chen L, Tay CJ, Li B. Flexible structured-light-based three--dimensional profile reconstruction method considering lens projection-imaging distortion. Appl Opt 2012;51(13):2419.
[22] Li K, Bu J, Zhang D. Lens distortion elimination for improving measurement accuracy of fringe projection profilometry. Opt Laser Eng 2016;85:53–64.
[23] Weng J, Cohen P, Herniou M. Camera calibration with distortion models and accuracy evaluation. IEEE T Pattern Anal 1992;14(10):965–80.
[24] Zhang Z. Determining the epipolar geometry and its uncertainty: a review. Int J Comput Vision 1998;27(2):161–95.